Journal Name

Supplementary material of "Probing the electronic structure and hydride occupancy of barium titanium oxyhydride through DFT-assisted solid-state NMR"

Rihards Aleksis,[1,2] Reji Nedumkandathil,[1] Wassilios Papawassiliou,[1] José P. Carvalho,[1] Aleksander Jaworski,[1] Ulrich Häussermann,[1] and Andrew J. Pell[1,3,a)]

[1)] *Department of Materials and Environmental Chemistry, Stockholm University, SE-106 91 Stockholm, Sweden*

[2)] *Latvian Institute of Organic Synthesis, Aizkraukles 21, Riga, LV 1006, Latvia*

[3)] *Centre de RMN à Très Hauts Champs de Lyon (UMR 5082 - CNRS, ENS Lyon, UCB Lyon 1), Universitè de Lyon, 5 rue de la Doua, 69100 Villeurbanne, France.*

(Dated: November 1, 2022)

[a)]Electronic mail: andrew.pell@ens-lyon.fr

SOLID-STATE NMR

The spectra for the quantification of the ^{2}H amount in the samples were acquired on the 2.5 mm probe spinning at 30 kHz using a rotor synchronized solid-echo sequence.[1,2] The experiments were acquired with 512 scans and recycle delay of 60, 40, 40 and 100 s for the $BTOD_{NAB}$, $BTOD_{CA}$, $BTOD_{EXCH}$ and glycine-($^{13}C_2$,^{15}N, 2,2-d_2) (95%, Sigma), respectively. Deuterated glycine was used as a reference sample with known ^{2}H composition. From the glycine sample mass and ^{2}H peak area the amount of deuterium in the sample was related to the signal integral, which was used to estimate the deuterium content in BTOD samples based on their mass and ^{2}H peak areas. For $BTOD_{EXCH}$ the deuterium amount was estimated only from the peak at -39 ppm.

The adiabatic shifting *d*-echo spectra at 290 K were acquired on the 2.5 mm probe under static conditions with 6 s recycle delay and 32 increments with 2048 transients per increment for $BTOD_{NAB}$, and 4 s recycle delay and 32 increments with 4096 transients per increment for $BTOD_{CA}$ and $BTOD_{EXCH}$. The adiabatic shifting *d*-echo spectra at 290 K were acquired on the 2.5 mm probe under static conditions with 6 s recycle delay and 32 increments with 2048 transients per increment for $BTOD_{NAB}$, and 4 s recycle delay and 32 increments with 4096 transients per increment for $BTOD_{CA}$ and $BTOD_{EXCH}$. The static adiabatic shifting *d*-echo spectrum at 420 K was acquired on the 4 mm probe with 4 s recycle delay and 32 increments with 1024 transients per increment, while the spectrum at 100 K was acquired on the LT 3.2 mm probe with 20 s recycle delay and 20 increments with 196 transients per increment. For the latter experiment the pulse sequence altered to select coherences using a cogwheel phase cycle.[3] The phase cycle was the same as for the phase-adjusted spinning sideband sequence.[4,5] The 2D spectra were processed in MATLAB[6] using in-house written scripts.

The longitudinal relaxation times T_1 of ^{2}H in $BTOD_{CA}$ at different temperatures was determined by saturation recovery using a sequence consisting of a saturation loop and a rotor-synchronized spin-echo.[7] The saturation recovery data were fit to a function of the form $I_0(1 - c\exp(-T_1/t))$ using Fitteia,[8] where T_1 is the longitudinal relaxation delay, t is time, I_0 is the signal intensity without saturation and c is a coefficient close 1 compensating for imperfect saturation.

The isotropic shift δ_{iso}, shift anisotropy $\Delta\delta_S$ and the asymmetry parameter η_S are defined

in terms of the shift tensor principal components $\tilde{\delta}_{ii}$ in the principal axis frame (PAF):

$$\delta_{\text{iso}} = \frac{1}{3}(\tilde{\delta}_{xx} + \tilde{\delta}_{yy} + \tilde{\delta}_{zz}), \tag{1}$$

$$\Delta\delta_{\text{S}} = \tilde{\delta}_{zz} - \delta_{\text{iso}}, \tag{2}$$

$$\eta_{\text{S}} = \frac{\tilde{\delta}_{yy} - \tilde{\delta}_{xx}}{\Delta\delta}. \tag{3}$$

The principal components $\tilde{\delta}_{ii}$ are arranged according to the Haeberlen convention as $|\tilde{\delta}_{zz} - \delta_{\text{iso}}| \geq |\tilde{\delta}_{xx} - \delta_{\text{iso}}| \geq |\tilde{\delta}_{yy} - \delta_{\text{iso}}|$.[9]

The quadrupolar coupling constant C_{Q} is defined as $C_{\text{Q}} = e^2qQ/h$, where eq is the anisotropy of the electric-field gradient tensor, eQ is the nuclear quadrupolar moment, and h is Planck's constant. The EFG anisotropy eq and asymmetry parameter are given in terms of the EFG principal components ($\tilde{V}_{ii}$) in the PAF as follows:

$$eq = \tilde{V}_{zz}, \tag{4}$$

$$\eta_{\text{Q}} = \frac{\tilde{V}_{yy} - \tilde{V}_{xx}}{\tilde{V}_{zz}}. \tag{5}$$

The principal components of the EFG tensor are arranged as $|\tilde{V}_{zz}| \geq |\tilde{V}_{xx}| \geq |\tilde{V}_{yy}|$ according to the Haeberlen convention.[9]

COMPUTATIONAL DETAILS

Quantum ESPRESSO

In Quantum ESPRESSO[10,11] the DFT calculations were carried out using the projector augmented-wave method[12]. The generalized gradient approximation exchange-correlation functional of Perdew, Burke, and Ernzerhof (PBE)[13] was used for the double occupied bandstate, whereas the combination of PBE with a U correction in the simplified rotationally invariant form was employed for polaron and single occupied bandstate.[14] The Hubbard-like term U was applied to Ti 3d orbitals.[15] The optimal value of $U = 2.7$ eV was parameterised following the approach reported previously,[16–18] in which U is chosen so that the total electronic energy is linearly dependent on the charge population of the polaron level (see Fig.S2). Standard projector augmented wave pseudopotentials were used available from QE.

All the calculations were performed on a $2 \times 2 \times 2$ supercell with a composition of $BaTiO_{2.875}H_{0.125}$ for polaron and single occupied bandstate and $BaTiO_{2.875}H_{0.25}$ for double

occupied bandstate. The plane wave basis set kinetic energy cut-off was set to 80 Ry and a $8 \times 8 \times 8$ Monkhorst-Pack grid was used for the Brillouin zone sampling. The calculations were spin polarized and used a Gaussian smearing with a width of $\sigma = 10^{-6}$ Ry was used for the polaron and single occupied bandstate, while $\sigma = 2$ mRy was used for the double occupied bandstate. The calculations were converged to energies within 10^{-9} and ionic relaxation forces within 10^{-5} Ry/Bohr. The EFG tensors were computed using the gauge including projector augmented wave (GIPAW) approach.[19]

WIEN2k

Additionally, the EFG calculations were performed by using the full-potential linearized augmented plane-wave method, as implemented in the WIEN2k package.[20] For all the calculations we used the structures optimised in Quantum ESPRESSO (see Fig.1). Spin polarised calculation with the PBE functional and a 2 mRy Gaussian smearing were employed for the double and single occupied bandstates, while PBE with a U correction of 2.7 eV was used for the polaron state. The k-mesh of 1000 point was used for the calculations. The plane wave basis set size was chosen by setting $\mathrm{RK_{max}} = 8$. Any other computational parameters, such as atomic sphere radii, potentials and wave functions within the atomic spheres were used as WIEN2k default settings.

ORCA

Furthermore, we computed the EFG parameters on the cluster models using with the ORCA code version 5.0.1[21] with the PBE0 functional[22–24]. The cluster models derived from the bandstate, polaron and double occupied optimised Quantum ESPRESSO structures by considering the first few coordination spheres surrounding the hydrogen atoms (see Fig.S4). The calculations all employed a very tight SCF convergence tolerance of 10^{-9} Hartree (verytightscf), and very tight integration grids (defgrid3). The radial grid (IntAcc) of the deuterium atoms was also increased to 12. The RIJCOSX approximation with def2/JK auxiliary basis-set for Coulomb-fitting was also employed. Orbital def2-QZVPP and def2-TZVP basis-sets[25] were used for the hydrogen atoms and the directly bonded titanium atoms, respectively. The orbital def2-SVP basis-set was used for the remaining atoms

in the clusters.

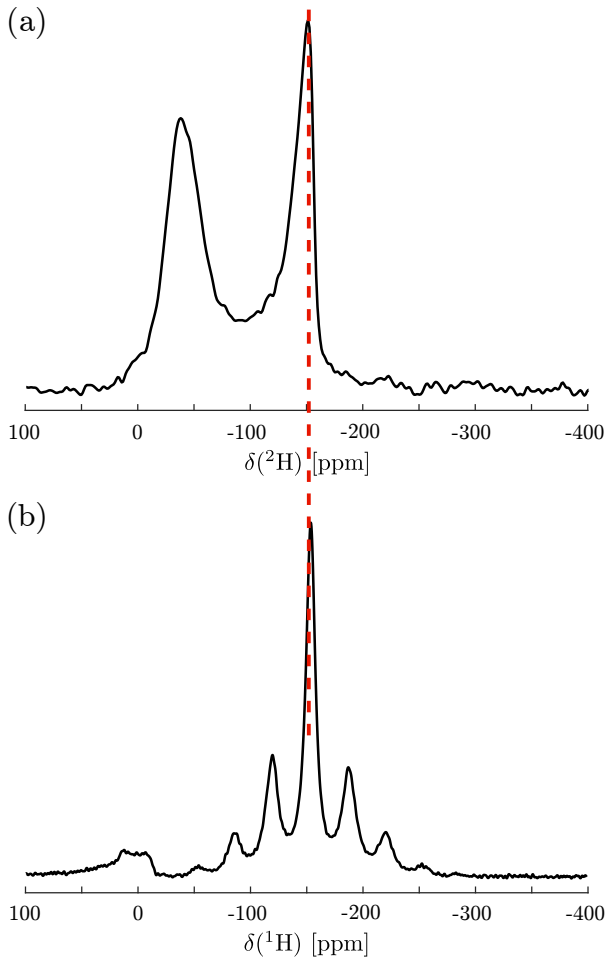

Figure S1. (a) shows the ^{2}H spectrum at 30 kHz MAS of $\mathrm{BTOD}_{\mathrm{EXCH}}$. (b) shows ^{1}H spectrum at 30 kHz MAS of TiH_2.

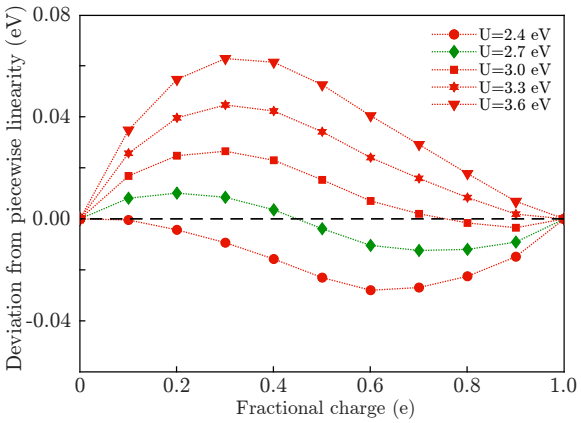

Figure S2. Deviation from linearity of the total electronic energy as a function of the charge of the system. The plots with suboptimal and optimal U values are given in red and green, respectively. The calculations were performed on a $2 \times 2 \times 2$ supercell with $BaTiO_{2.875}H_{0.125}$ composition in the polaronic state.

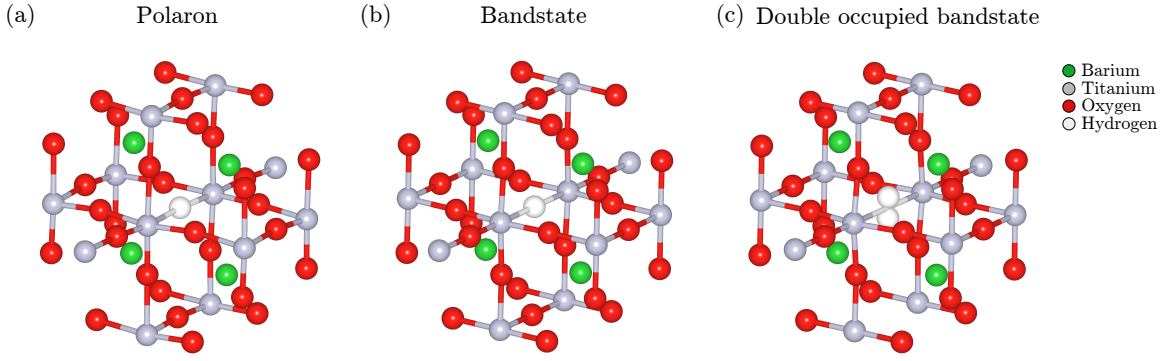

Figure S3. Cluster models used for calculations in ORCA. From left to right the cluster structures of the polaronic state (a), bandstate (b) and double occupied bandstate (c).

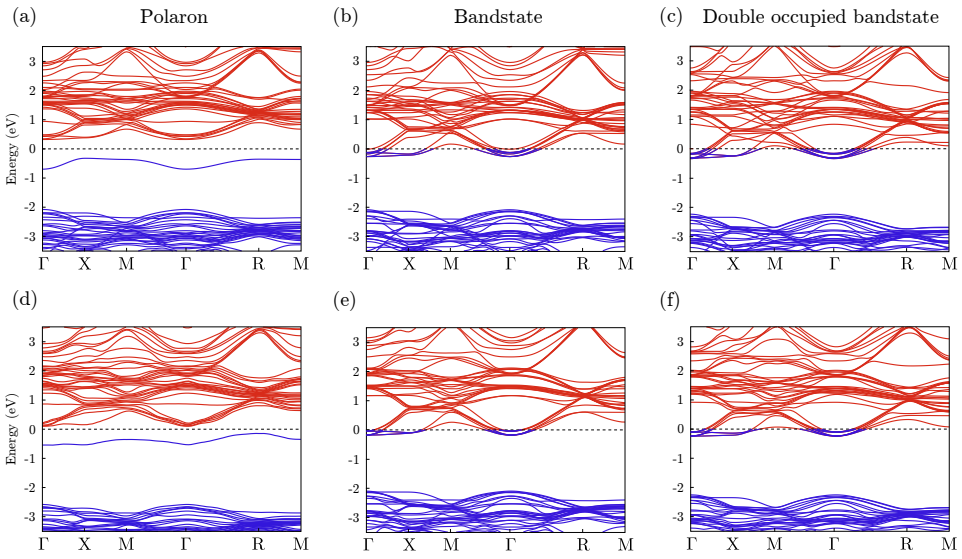

Figure S4. Electronic band structure of polaronic state (a), bandstate (b), and double occupied bandstate (c) obtained using Quantum ESPRESSO. The electronic band structures of the polaronic state (d), bandstate (e) and double occupied bandstate (f) calculated in WIEN2k. The blue and red colours represent occupied and unoccupied levels, respectively.

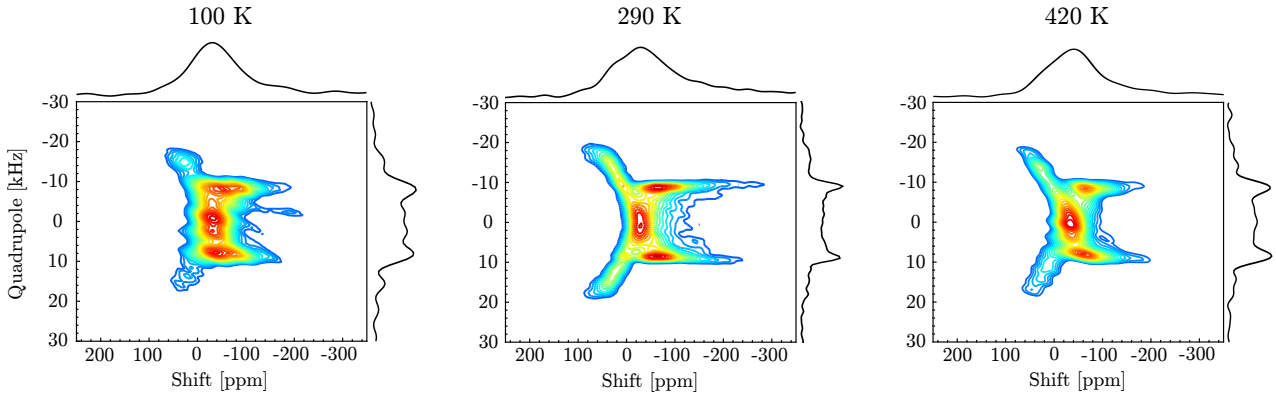

Figure S5. 2D static shifting *d*-echo NMR spectra of $BTOD_{CA}$ at different temperatures. From left to right the 2D adiabatic shifting *d*-echo spectra are shown acquired at 100 K, 290 K and 420 K.

REFERENCES

[1]J. Davis, K. Jeffrey, M. Bloom, M. Valic and T. Higgs, *Chem. Phys. Lett.*, 1976, **42**, 390–394.

[2]S. Antonijevic and S. Wimperis, *J. Magn. Reson.*, 2003, **164**, 343–350.

[3]M. H. Levitt, P. Madhu and C. E. Hughes, *J. Magn. Reson.*, 2002, **155**, 300 – 306.

[4]N. Ivchenko, C. E. Hughes and M. H. Levitt, *J. Magn. Reson.*, 2003, **164**, 286–293.

[5]R. Aleksis and A. J. Pell, *J. Chem. Phys.*, 2021, **155**, 094202.

[6]D. J. Higham and N. J. Higham, *MATLAB guide*, SIAM, 2016.

[7]E. L. Hahn, *Phys. Rev.*, 1950, **80**, 580.

[8]P. J. Sebastião, *Eur. J. Phys.*, 2013, **35**, 015017.

[9]U. Haeberlen, *Advances in magnetic resonance*, Academic Press, 1976, vol. 1.

[10]P. Giannozzi, S. Baroni, N. Bonini, M. Calandra, R. Car, C. Cavazzoni, D. Ceresoli, G. L. Chiarotti, M. Cococcioni, I. Dabo *et al.*, *J. Phys.: Condens. Matter*, 2009, **21**, 395502.

[11]P. Giannozzi, O. Andreussi, T. Brumme, O. Bunau, M. B. Nardelli, M. Calandra, R. Car, C. Cavazzoni, D. Ceresoli, M. Cococcioni *et al.*, *J. Phys.: Condens. Matter*, 2017, **29**, 465901.

[12]P. E. Blöchl, *Phys. rev. B*, 1994, **50**, 17953.

[13]J. P. Perdew, K. Burke and M. Ernzerhof, *Phys. Rev. Lett.*, 1996, **77**, 3865.

[14]M. Cococcioni and S. De Gironcoli, *Phys. Rev. B*, 2005, **71**, 035105.

[15]V. I. Anisimov, J. Zaanen and O. K. Andersen, *Phys. Rev. B*, 1991, **44**, 943–954.

[16]E. J. Granhed, A. Lindman, C. Eklöf-Österberg, M. Karlsson, S. F. Parker and G. Wahnström, *J. Mater. Chem. A*, 2019, **7**, 16211–16221.

[17]S. Lany and A. Zunger, *Phys. Rev. B*, 2009, **80**, 085202.

[18]P. Erhart, A. Klein, D. Åberg and B. Sadigh, *Phys. Rev. B*, 2014, **90**, 035204.

[19]T. Charpentier, *Solid State Nucl. Magn. Reson.*, 2011, **40**, 1–20.

[20]P. Blaha, K. Schwarz, F. Tran, R. Laskowski, G. K. Madsen and L. D. Marks, *J. Chem. Phys.*, 2020, **152**, 074101.

[21]F. Neese, *Wiley Interdiscip. Rev. Comput. Mol. Sci.*, 2012, **2**, 73–78.

[22]C. Adamo and V. Barone, *J. Chem. Phys.*, 1999, **110**, 6158–6170.

[23]R. Bjornsson and M. Bühl, *Dalton Trans.*, 2010, **39**, 5319–5324.

[24]R. Bjornsson and M. Bühl, *Chem. Phys. Lett.*, 2013, **559**, 112–116.

[25]F. Weigend and R. Ahlrichs, *Phys. Chem. Chem. Phys.*, 2005, **7**, 3297–3305.